

An Improved Particle Swarm Optimization (PSO)–Based MPPT for PV With Reduced Steady-State Oscillation

Kashif Ishaque, Zainal Salam, *Member, IEEE*, Muhammad Amjad, and Saad Mekhilef, *Member, IEEE*

Abstract—This paper proposes an improved maximum power point tracking (MPPT) method for the photovoltaic (PV) system using a modified particle swarm optimization (PSO) algorithm. The main advantage of the method is the reduction of the steady-state oscillation (to practically zero) once the maximum power point (MPP) is located. Furthermore, the proposed method has the ability to track the MPP for the extreme environmental condition, e.g., large fluctuations of insolation and partial shading condition. The algorithm is simple and can be computed very rapidly; thus, its implementation using a low-cost microcontroller is possible. To evaluate the effectiveness of the proposed method, MATLAB simulations are carried out under very challenging conditions, namely step changes in irradiance, step changes in load, and partial shading of the PV array. Its performance is compared with the conventional Hill Climbing (HC) method. Finally, an experimental rig that comprises of a buck–boost converter fed by a custom-designed solar array simulator is set up to emulate the simulation. The software development is carried out in the Dspace 1104 environment using a TMS320F240 digital signal processor. The superiority of the proposed method over the HC in terms of tracking speed and steady-state oscillations is highlighted by simulation and experimental results.

Index Terms—Buck–boost converter, Hill Climbing (HC), maximum power point tracking (MPPT), partial shading, particle swarm optimization (PSO), photovoltaic (PV) system.

I. INTRODUCTION

SOLAR photovoltaic (PV) is envisaged to be a popular source of renewable energy due to several advantages, notably low operational cost, almost maintenance free and environmentally friendly. Despite the high cost of solar modules, PV power generation systems, in particular the grid-connected type, have been commercialized in many countries because of its potential long-term benefits [1]–[6]. Furthermore, generous

financial schemes, for example, the feed-in tariff [7] and subsidized policies [8], have been introduced by various countries, resulting in rapid growth of the industry. To optimize the utilization of large arrays of PV modules, maximum power point tracker (MPPT) is normally employed in conjunction with the power converter (dc–dc converter and/or inverter). The objective of MPPT is to ensure that the system can always harvest the maximum power generated by the PV arrays. However, due to the varying environmental condition, namely temperature and solar insolation, the P – V characteristic curve exhibits a maximum power point (MPP) that varies nonlinearly with these conditions—thus posing a challenge for the tracking algorithm.

To date, various MPP tracking methods have been proposed [9]. These techniques vary in complexity, accuracy, and speed. Each method can be categorized based on the type of the control variable it uses: 1) voltage, 2) current, or 3) duty cycle. For the voltage- and current-based techniques, two approaches are used. The first one is the observation of MPP voltage V_{MP} or current I_{MP} with respect to the open circuit voltage V_{OC} [10] and short circuit current I_{SC} , respectively [11]. Since this method approximates a constant ratio, its accuracy cannot be guaranteed. Consequently, the tracked power would most likely be below the real MPP, resulting in significant power loss [12]. The second approach is to obtain the information on the actual operating point of the PV array (i.e., voltage and current) and these points are updated according to the variation in environmental conditions. The most popular technique is the perturb and observe (P&O) method. It is based on the perturbation of voltage (or current) using the present P and previous P_{old} operating power, respectively. If P is improved, the direction of perturbation is retained; otherwise, the direction is reversed accordingly.

Despite the simplicity of the algorithm, the performance of P&O method is heavily dependent on the tradeoff between the tracking speed and the oscillations that occurs around the MPP [13]. A small perturbation reduces the oscillations but at the expense of tracking speed, or vice versa. Another major drawback of P&O is that during rapid fluctuations of insolation, the algorithm is very likely to lose its direction while tracking the true MPP. Several improvements are proposed to address this issue—mainly by considering adaptive perturbation. However, these techniques are not fully adaptive and hence are not very effective [14]. Moreover, under special condition such as partial shading and modules irregularities, these methods often fail to track the true MPP because the PV curves are characterized by multiple peaks (several local and one global). Since the P&O algorithm could not distinguish the correct peak, its usefulness

Manuscript received September 14, 2011; revised September 21, 2011; accepted January 8, 2012. Date of current version April 20, 2012. Recommended for publication by Associate Editor M. Liserre.

K. Ishaque was with the Universiti Teknologi Malaysia, Johor Bahru 81310, Malaysia. He is now with the Department of Electronics Engineering, Karachi Institute of Economics and Technology, Karachi 75190, Pakistan (e-mail: kashif.ishaque@pafkiet.edu.pk).

Z. Salam (corresponding author) and M. Amjad are with the Universiti Teknologi Malaysia, Johor Bahru 81310, Malaysia (e-mail: zainals@fke.utm.my; Muhammad.Amjad@iub.edu.pk).

S. Mekhilef is with the University of Malaya, Kuala Lumpur 50603, Malaysia (e-mail: saad@um.edu.my).

Color versions of one or more of the figures in this paper are available online at <http://ieeexplore.ieee.org>.

Digital Object Identifier 10.1109/TPEL.2012.2185713

under such conditions diminishes rapidly [12]. Another method is the incremental conductance (IC) which is based on incrementally comparing the ratio of derivative of conductance with the instantaneous conductance [15]. Although IC does not suffer the lost of tracking direction, it inherits the same problems as P&O, namely the inevitable tradeoff between the MPPT speed and oscillation. Several improved IC techniques are proposed; for instance, the authors in [4] managed to improve the oscillations at MPP but during rapid fluctuation of environmental conditions, the tracking speed reduces significantly.

The third category of MPPT techniques is characterized by the duty cycle control. In the literature, it is known as Hill Climbing (HC) or direct control method. As the latter name implies, HC operates by directly updating the converter's duty cycle [16]. The approach greatly simplifies the control structure as it eliminates the need for the proportional integral (PI) or hysteresis controller. In principle, it works on the same concept as P&O, but instead of perturbing the voltage or current, it updates the operating point of the PV array by perturbing the duty cycle. With the absence of the PI loop, the implementation of HC is greatly simplified. Consequently, this method is extensively used in PV systems [17]. However, it also suffers with same drawbacks inherited by P&O.

In an effort to overcome aforementioned disadvantages, several pieces of research have used artificial intelligence approach such as fuzzy logic controller (FLC) [18] and neural network (NN) [19]. Although these methods are effective in dealing with the nonlinear characteristics of the $I-V$ curves, they require extensive computation. For example, FLC has to deal with fuzzification, rule base storage, inference mechanism, and defuzzification operations. For NN, the large amount of data required for training are a major source of constraint. Furthermore, as the operating conditions of the PV system vary continuously, MPPT has to respond to changes in insolation and temperature variations in real time. Clearly, a low-cost processor cannot be employed in such a system.

An alternative approach is to employ evolutionary algorithm (EA) techniques. Due to its ability to handle nonlinear objective functions [20], [21], EA is envisaged to be very effective to deal with the MPPT problem. Among the EA techniques, particle swarm optimization (PSO) is highly potential due to its simple structure, easy implementation, and fast computation capability [22]. Since PSO is based on search optimization, in principle, it should be able to locate the MPP for any type of $P-V$ curve regardless of environmental variations. Realizing these advantages, several researchers have employed this technique to improve the MPP tracking [23]–[26]. In [23] and [24], the authors have added various extra coefficients in the conventional PSO searching scheme equations, thus increasing the computational burden of the algorithm. The authors in [25] formulated an analytical expression of the objective functions based on PV current, solar insolation, and temperature; then, PSO is utilized to track the MPP. However, it is not shown that the expression is equivalent to the real operating power; hence, tracking of the correct MPP is not certain—raising the questions about the effectiveness of this method. In [26], the authors employed PSO to optimize the parameters for the LC filter in the microgrid

system. Since the method specifically focused on the grid side, it is of little interest because the concern of the majority of the MPPT work is on the input side.

Interestingly, one important feature of the PSO which is ignored by researchers [23]–[26] is the fact that once the particles find the MPP, their associated velocity becomes very low or practically null. This advantage is overlooked because the previous work has not attempted to use PSO in conjunction with the direct duty cycle control. If the two are combined, at MPP, the duty cycle can be maintained at constant value and this in turn diminishes the steady-state oscillations that typically exist in conventional MPPT techniques. Consequently, power loss due to the oscillation is eliminated and system efficiency increases.

To capitalize that particular advantage, this paper proposes an improved MPPT method based on a modified PSO algorithm. It will be shown that the proposed MPPT has a similar structure to the conventional HC; therefore, a direct duty cycle control can be utilized. The main feature of the proposed method is the absence of steady-state oscillation at MPP. It also has the ability to track the MPP for the extreme environmental condition, e.g., large fluctuations of insolation and partial shading condition. Compared to other conventional MMPT techniques, it has a faster tracking speed. Furthermore, the algorithm is simple and can be computed very rapidly; thus, its implementation using a low-cost controller is possible.

The remainder of this paper is organized as follows. Section II discusses the modeling of the PV module and array based on the work published in [27]. This would be the basis for the simulation work that ensues. In Section III, the conventional HC method is briefly introduced. Section IV describes the overview of the PSO and how it is applied to track the MPP. In addition, the modified PSO algorithm used to improve the tracking performance is also outlined. Section V describes the overview of the overall simulation and experimental set-up. For simulation, a comprehensive PV simulator developed in [28] is utilized. To validate the idea, the algorithm is implemented using a prototype buck–boost converter fed by a custom-designed solar array simulator. The software development is carried out in the DSpace 1104 environment with a TMS320F240 digital signal processor. Section VI compares the results obtained using proposed PSO and HC methods. Finally, the conclusion is made in the last section.

II. MODELING OF THE PV MODULE AND ARRAY

A. Modeling PV Module

Among various modeling methods of the PV module, the two-diode model, as depicted in Fig. 1(a), is known to be the more accurate one. The output current of the module can be described as

$$I = I_{PV} - I_{d1} - I_{d2} - \left(\frac{V + IR_s}{R_p} \right) \quad (1)$$

where

$$I_{d1} = I_{o1} \left[\exp \left(\frac{V + IR_s}{a_1 V_{T1}} \right) - 1 \right] \quad (2)$$

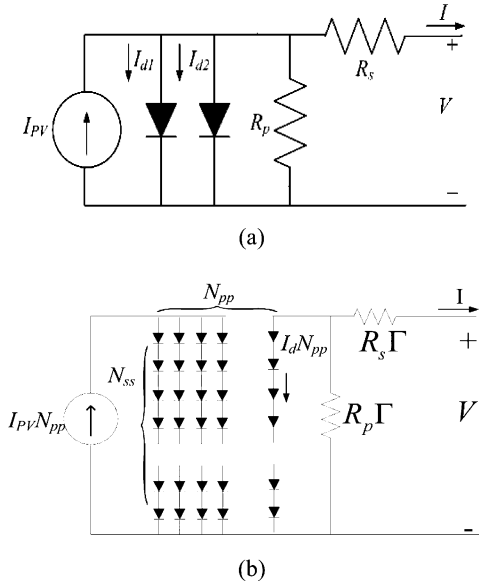


Fig. 1. (a) Two-diode model of the PV cell. (b) Series parallel combination of the PV array.

and

$$I_{d2} = I_{o2} \left[\exp \left(\frac{V + IR_s}{a_2 V_{T2}} \right) - 1 \right] \quad (3)$$

where I_{PV} is the current generated by the incidence of light; and I_{o1} and I_{o2} are the reverse saturation currents of diode 1 and diode 2, respectively. The I_{o2} term is introduced to compensate for the recombination loss in the depletion region as described in [29]. Other variables are defined as follows: V_{T1} and V_{T2} (both equal to $N_s kT/q$) are the thermal voltages of the PV module having N_s cells connected in series, q is the electron charge ($1.60217646 \times 10^{-19}$ C), k is the Boltzmann constant ($1.3806503 \times 10^{-23}$ J/K), and T is the temperature of the p-n junction in Kelvin. Variables a_1 and a_2 represent the diode ideality constants, respectively. Although greater accuracy can be achieved using this model than the single-diode model, it requires the computation of seven parameters, namely I_{PV} , I_{o1} , I_{o2} , R_p , R_s , a_1 , and a_2 .

Recently, a fast and simple two-diode model has been proposed in [27]. In this model, the simplified current equation is developed and is given as

$$I = I_{PV} - I_o (I_p + 2) - \left(\frac{V + IR_s}{R_p} \right) \quad (4)$$

where

$$I_p = \exp \left(\frac{V + IR_s}{V_T} \right) + \exp \left(\frac{V + IR_s}{(p-1)V_T} \right) \quad (5)$$

and

$$p = 1 + a_2. \quad (6)$$

The model only requires five parameters to be computed with no loss of accuracy.

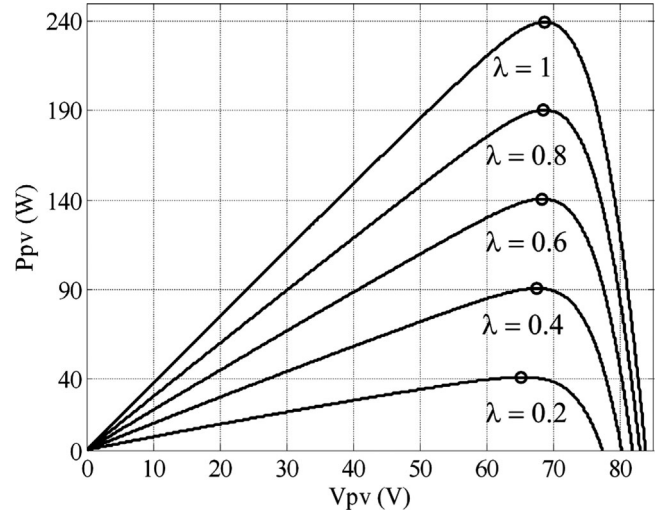


Fig. 2. P - V curves for MSX-60 in 4×1 configuration for different irradiation levels.

TABLE I

PARAMETERS OF THE MSX-60 PV MODULE AT STC: TEMPERATURE = 25 °C, AIR MASS = 1.5, AND INSOLATION = 1000 W/m²

Peak Power(W), P_{mpp}	60
Peak power voltage(V), V_{mpp}	17.1
Peak power current(A), I_{mpp}	3.5
Open circuit voltage(V), V_{oc}	21.1
Short circuit current(A), I_{sc}	3.8
Temperature coefficient of current (mA/°C), K_i	0.003
Temperature coefficient of voltage (mV/°C), K_V	-0.08
Number of series cells, N_s	36

B. Modeling of the PV Array

In a typical installation of a large PV power generation system, the modules are configured in a series-parallel structure (i.e., $N_{ss} \times N_{pp}$ modules), as depicted in Fig. 1(b). To handle such cases, the output current equation in (4) has to be modified as follows:

$$I = N_{pp} \{ I_{PV} - I_o (I_p + 2) \} - \left(\frac{V + IR_s \Gamma}{R_p \Gamma} \right) \quad (7)$$

where

$$I_p = \exp \left(\frac{V + IR_s \Gamma}{V_T N_{ss}} \right) + \exp \left[\frac{V + IR_s \Gamma}{(p-1)V_T N_{ss}} \right] \quad (8)$$

and

$$\Gamma = \frac{N_{ss}}{N_{pp}} \quad (9)$$

where I_{PV} , I_o , R_p , R_s , p are the parameters of the individual module. Fig. 2 shows the P - V curves for a commercial PV module (MSX-60) configured in a 4×1 PV array. The parameters of this particular module under the standard test condition (STC) are shown in Table I.

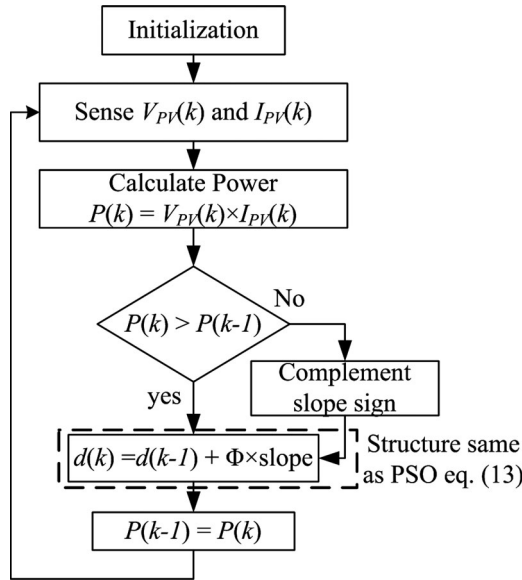


Fig. 3. Flowchart of the conventional HC method.

III. CONVENTIONAL HC METHOD

To obtain the maximum power from the PV modules, MPPT is normally employed. Over the years, various MPPT methods are proposed; for example, P&O, IC, HC, NN, and FLC [4], [9], [12], [15]–[19], [22]. In particular, the conventional HC method is interesting as the duty cycle of the power converter can be varied directly [16]. This can be explained with the help of a flowchart as shown in Fig. 3. The algorithm periodically updates the duty cycle $d(k)$ by a fixed step size Φ with the direction of increasing power. The perturbation direction is reversed if $P(k) < P(k-1)$, an indication that the tracking is not moving toward the MPP. This can be described by the following equation:

$$d_{\text{new}} = \begin{cases} d_{\text{old}} + \Phi & \text{if } P > P_{\text{old}} \\ d_{\text{old}} - \Phi & \text{if } P < P_{\text{old}}. \end{cases} \quad (10)$$

A clear advantage of this algorithm is that the MPPT algorithm does not require proportional (P) or proportional integral (PI) action, which is normally employed to control the duty cycle with reference to voltage or current. In this case, the duty cycle directly feeds the power converter.

IV. PSO-BASED MPPT

A. General Overview of PSO

PSO is a stochastic, population-based EA search method, modeled after the behavior of bird flocks [30]. The PSO algorithm maintains a swarm of individuals (called particles), where each particle represents a candidate solution. Particles follow a simple behavior: emulate the success of neighboring particles and its own achieved successes. The position of a particle is, therefore, influenced by the best particle in a neighborhood P_{best} as well as the best solution found by all the particles in the entire population G_{best} . The particle position x_i is adjusted

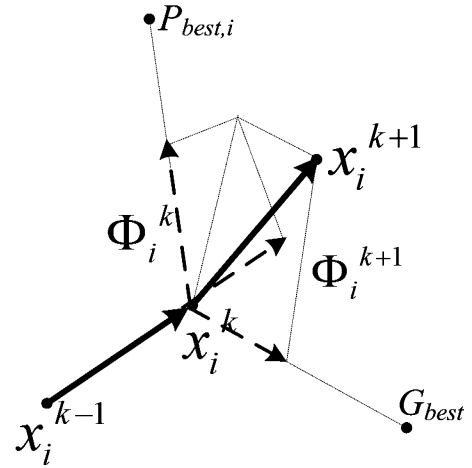


Fig. 4. Movement of particles in the optimization process.

using

$$x_i^{k+1} = x_i^k + \Phi_i^{k+1} \quad (11)$$

where the velocity component Φ_i represents the step size. The velocity is calculated by

$$\Phi_i^{k+1} = w\Phi_i^k + c_1r_1\{P_{\text{best},i} - x_i^k\} + c_2r_2\{G_{\text{best}} - x_i^k\} \quad (12)$$

where w is the inertia weight, c_1 and c_2 are the acceleration coefficients, $r_1, r_2 \in U(0, 1)$, $P_{\text{best},i}$ is the personal best position of particle i , and G_{best} is the best position of the particles in the entire population. Fig. 4 shows the typical movement of particles in the optimization process.

If position is defined as the actual duty cycle while velocity shows the perturbation in the present duty cycle, then (11) can be rewritten as

$$d_i^{k+1} = d_i^k + \Phi_i^{k+1}. \quad (13)$$

From (10) and (13), it can be seen that both HC and PSO algorithms have an equivalent structure. However, for the case of PSO, resulting perturbation in the present duty cycle depends on $P_{\text{best},i}$ and G_{best} . If the present duty cycle is far from these two duty cycles, the resulting change in the duty cycle will also be large, and vice versa. Therefore, PSO can be thought of as an adaptive form of HC. In the latter, the perturbation in the duty cycle is always fixed but in PSO it varies according to the position of the particles. With proper choice of control parameters, a suitable MPPT controller using PSO can be easily designed.

B. Application of PSO for MPPT

To illustrate the application of the PSO algorithm in tracking the MPP using the direct control technique, first a solution vector of duty cycles with Np particles is determined, i.e.

$$x_i^k = d_g = [d_1, d_2, d_3, \dots, d_j] \quad (14)$$

$$j = 1, 2, 3, \dots, Np.$$

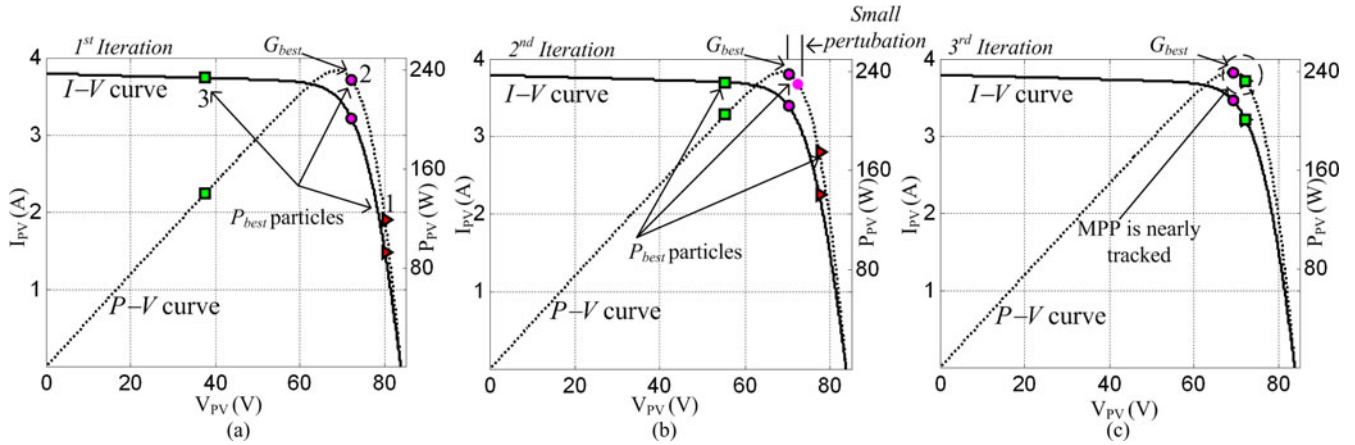


Fig. 5. PSO particle movements in searching for the MPP.

The objective function is defined as

$$P(d_i^k) > P(d_i^{k-1}). \quad (15)$$

To start the optimization process, the algorithm transmits three duty cycles d_i ($i = 1, 2, 3$) to the power converter. In Fig. 5, duty cycles d_1 , d_2 , and d_3 are marked with triangular, circular, and square points, respectively. These duty cycles served as the P_{besti} in the first iteration. Among these, d_2 is the G_{best} that gives the best fitness value (which is the array power), as illustrated by Fig. 5(a). In the second iteration, the resulting velocity is only due to the G_{best} term. The $(P_{besti} - d(i))$ factor in (12) is zero. Furthermore, the velocity of G_{best} particle (d_2) is zero due to the $(G_{best} - d(2))$ factor in (12) is zero. This results in a zero velocity and accordingly the duty cycle is unchanged. As a result, this particle will not contribute in the exploration process. To avoid such situation, a small perturbation in duty cycle is allowed, as shown in Fig. 5(b), to ensure the change in fitness value. Fig. 5(c) shows the particles movement in the third iteration. Due to the fact that all the duty cycles in the previous iteration attain a better fitness value, the velocity direction of these particles remains unchanged and subsequently they move toward G_{best} along the same direction. In the third iteration, all duty cycles (d_i , $i = 1, 2, 3$) arrive at MPP with a low value of velocity. In the subsequent iteration, due to very low velocity, the value of the duty cycle is approaching a constant. Therefore, the operating point will be maintained and the oscillation around the MPP diminishes.

C. Tracking During Partial Shading

When the PV array is operating in a uniform solar insolation, the resulting $P-V$ characteristic curve of the array exhibits a single MPP. However, under partial shading, the $P-V$ curves are characterized by multiple peaks, i.e., with several local and one global peak as depicted in Fig. 6. In this example, the $I-V$ curve is characterized by four stairs, while the $P-V$ curve is characterized by four peaks. The latter are labeled as $P1$, $P2$, $P3$, and $P4$. It can be observed that the time derivative of power dP/dV is zero for the global as well as all the local peaks. Furthermore, the slope at its right and left sides has the

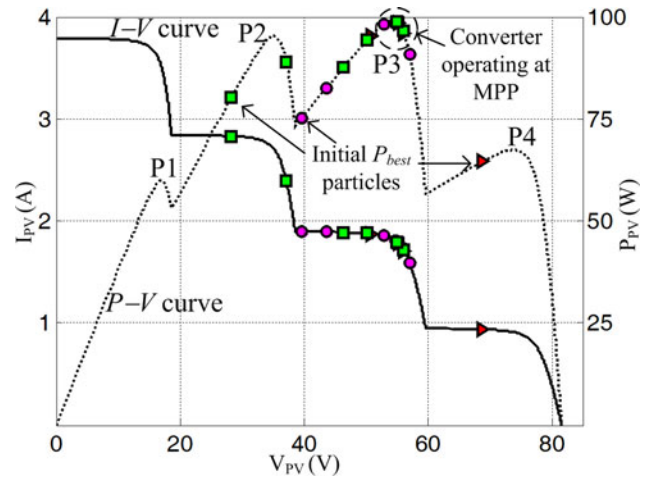


Fig. 6. MPPT tracking by PSO during partial shading.

same signs. Since all conventional MPPT methods are based on the slope and sign value of dP/dV , the algorithm could not distinguish the local ($P1$, $P2$, and $P4$) and global peaks ($P3$) correctly. It is very likely that the MPPT is being forced to trap into the local peak, resulting in reduced output power and thus greatly deteriorates the efficiency of the PV system.

On the other hand, since the PSO method works on the basis of search technique, the global peak can be tracked without any difficulty. Fig. 6 depicts the tracking capability of PSO during partial shading. Similar to the previous $P-V$ curve (see Fig. 5), the proposed method transmits three duty cycles, which serve as P_{best} particles. It can be seen that the voltage and current contributing to these initial duty cycles (P_{besti}) are away from the global peak ($P3$). But in the later phases of iterations, it successfully finds the global peak, $P3$.

D. Modified PSO Structure

In the case of slow variation in the solar insolation, a proper initialization of duty cycles in PSO is very critical. In this case, a change in the duty cycle from the previous one should be

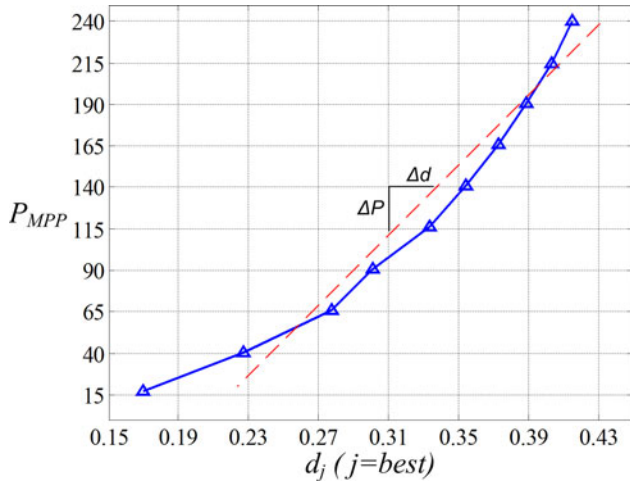


Fig. 7. Relationship between the G_{best} duty cycle and P_{MPP} .

small to track the MPP. Thus, due to the initialization, when the change in the duty cycle is large, the particles will have to search a large area of the $P-V$ curve. However, MPP will still be tracked at the expense of large fluctuations in the operating point. Consequently, certain amount of energy will be wasted during the exploration process. Another serious problem needs to be considered is when the change in the insolation is small (as discussed earlier) but occurs very rapidly. In this scenario, the tracking needs to be fast enough to follow the rapid change. However, the large change in the duty cycles does not allow for the duty cycles to follow the new MPP very accurately [22]. On the other hand, a large change in the operating point can also occur due to a large change in insolation, for example, during the partial shading condition [31]. In this case, if the change in the duty cycle is small, the convergence toward the MPP could be slow. This could be more critical for the case of partial shading. As duty cycles are not allowed to explore a larger area of the $P-V$ curve, the final MPP could settle at a local instead of global peak.

To address these two issues, the conventional PSO need to be modified. The duty cycles are initialized in two phases. First, the previous duty cycles are decreased or increased linearly (according to the change in array power) by a factor K_1 . It can be noted that once the PSO reaches MPP, all the three duty cycles are at almost the same value due to the zero velocity. In order to search the $P-V$ curve for the new MPP, the second step involves the perturbation of two extreme duty cycles (d_1 and d_3) in positive and negative directions with a constant value of K_2 .

Fig. 7 proposes a systematic method to estimate value of K_1 . In this figure, a relationship between the array maximum power P_{MPP} and the corresponding duty cycle G_{best} is plotted. G_{best} is the corresponding duty cycle which is responsible for the dc-dc converter to operate at P_{MPP} . The response is obtained by reducing the solar insolation from $\lambda = 1$ to $\lambda = 0.1$ with a step size of 0.1. It can also be seen that there exists a quadratic relationship between P_{MPP} and d_{best} . More importantly, an approximate linear correlation, shown by the dotted line in Fig. 7, between the change in array power and duty cycle

can be obtained using

$$d_{\text{new}} = d_{\text{old}} - \frac{1}{K_1} (P_{\text{old,MPP}} - P_{\text{MPP}}) \quad (16)$$

where d_{old} is the previous G_{best} duty cycle and $K_1 = \Delta P_{\text{MPP}} / \Delta d$ is the slope of the linear segment.

An attractive advantage of (15) is that with the change in the environmental condition, the new duty cycles will be varied according to the change in operating power but its value will always be very close to the new best duty cycle. Hence, the reinitialization of duty cycles will not result in unnecessary exploring of the $P-V$ curve. This allows for the new MPP to be tracked very rapidly.

It should be noted that the aforementioned analyses are carried out with decreasing insolation, i.e., from $\lambda = 1$ to $\lambda = 0.1$. The reducing insolation will always result in the load line being on the left of the maximum PV array voltage V_{MPP} of the $I-V$ curve. Consequently, a larger change in the operating power will occur. However, this is not true for the case when the insolation increases from a low to high value, for example, from $\lambda = 0.4$ to $\lambda = 1$. This is due to the fact that for an increasing insolation, the load line will always be at the right side of V_{MPP} . Since the difference between V_{MPP} and V_{OC} is not large, a low change in operating power is observed. Therefore, if the same value of K_1 is used for this case, d_{old} will not be properly scaled. As a result, PSO will utilize more iteration to reach at MPP. To avoid such problem, different pairs of K_1 values are used for each of the two cases. The value of K_1 is selected accordingly using the following relationship:

$$K_1 = \begin{cases} K_1 & \text{if } \Delta P > 0 \\ \frac{K_1}{2} & \text{if } \Delta P < 0 \end{cases} \quad (17)$$

where

$$\Delta P = (P - P_{\text{old}}). \quad (18)$$

Note that $\Delta P > 0$ and $\Delta P < 0$ indicate decreasing and increasing insolation, respectively.

To perturb the new duty cycle which is obtained through (16), d_1 and d_3 are equally displaced in positive and negative directions, respectively by a factor of K_2 i.e.,

$$d_{i,\text{new}}^k = [d_1 - K_2, d_2, d_3 + K_2] \text{ for } K_2 \geq 0.05. \quad (19)$$

The value of 0.05 in (19) is selected so that the fluctuations in the operating power of the PV array will not be too large. However, in some special cases, such as partial shading in which there exist multiple peaks (several local with one global), this number can be increased based on the operating voltage (in the range of 30–85% of V_{OC} voltage of the PV array [12]). This is to allow the PSO algorithm to explore a wider range of the $I-V$ curve so that global peak could be tracked.

It should also be noted that even if the duty cycle computed through (16) is nowhere near to the final best duty cycle, but due to the perturbation factor K_2 , at least one of d_i ($i = 1, 2, 3$) will still be close to the best duty cycle. Hence, (16) and (19) always ensure a fast tracking. Fig. 8 shows the complete flowchart of the proposed method.

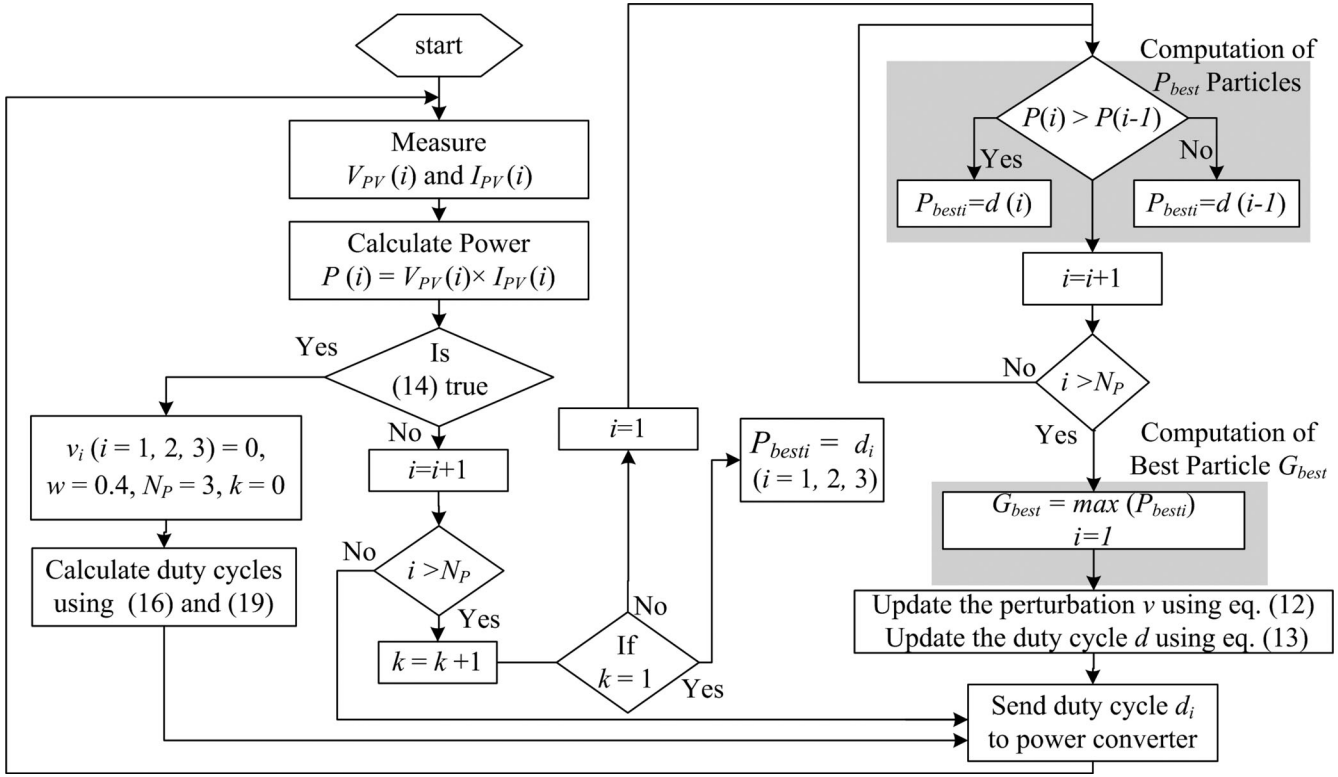


Fig. 8. Complete flowchart of the proposed method.

E. Advantages of the Proposed PSO Method

The proposed method offers several advantages compared to other MPPT techniques.

- 1) Equation (10) shows that the perturbation in duty cycle is computed by two difference terms: the difference between the previous duty cycle $d_i(k)$ and the local best particles P_{besti} , and the difference between the previous duty cycle $d_i(k)$ and the global best particle G_{best} . Thus, the power converter tracks the two best P_{besti} and G_{best} at the same time. As a result, the tracking spaces are searched to obtain an optimal solution with a faster speed.
- 2) Once the particle reaches MPP, the velocity of particles is practically zero. Hence, at steady state no oscillations will be seen. These steady-state oscillation (normally present in HC) are very critical because it is one of the major reasons for the reduced MPPT efficiency [17].
- 3) In the case of rapid fluctuations in the environmental conditions, the HC method can lose the direction of new MPP and tracking could be driven into a wrong direction. This is one of the major problems of the HC method [18]. However, the proposed method works on three duty cycles. Since the operating power information is obtained from all three duty cycles, it never loses the direction of MPP—in rapid fluctuations.
- 4) In the condition of partial shading, the P – V characteristic curve is characterized by multiple peaks. As a result, the HC method is most likely to trap at local maxima. On the other hand, the PSO method works based on a searching scheme. Hence, it can still track the global peak correctly.

V. SIMULATION RESULTS

Fig. 9 shows the MATLAB–Simulink simulation model of the PV system used in this study. The buck–boost dc/dc converter is utilized due to several reasons [32], namely 1) it exhibits superior characteristics with respect to the performance of PV array's MPP; and 2) it follows the MPP at all times, regardless of the solar insolation, the array temperature, and the connected load. The converter is designed for continuous inductor current mode with the following specifications: $C_1 = 470 \mu\text{F}$, $C_2 = 220 \mu\text{F}$, $L = 1 \text{ mH}$, and 50-kHz switching frequency. The PV modules utilized are the MSX60 configured in a 4×1 array. The key specifications of the module are shown in Table I.

To implement the PSO algorithm, the following control parameters are used in both simulation and experiment: $C_1 = 1.2$, $C_2 = 1.6$, $w = 0.4$, and $P_{thr} = 1.5\%$. These parameters are obtained in [22]. To avoid large fluctuations in the operating point of the PV array, the value of K_2 is chosen to be 0.05 as suggested in (19). The array is configured as 4×1 (series–parallel), with each module rated at 60 W. The total power of the array is 240 W at STC. Fig. 7 is used to estimate the value of K_1 . Using (16), the approximated values of K_1 are computed as 675 and 1350 for increasing and decreasing insolation, respectively.

Simulations are carried out using the comprehensive PV system simulator developed in [28]. The sampling time for the MPPT controller is very crucial, i.e., the PV system must reach the steady state (MPP) before the next sampling begins. In accordance to the work published in [32], the sampling interval is chosen to be 0.1 s.

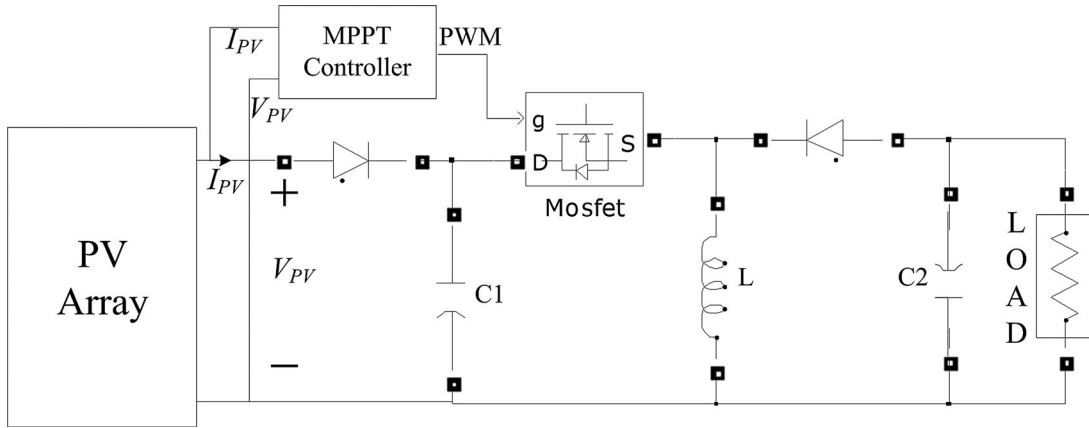


Fig. 9. MATLAB-Simulink simulation model for the PV system with the buck-boost converter and MPPT controller.

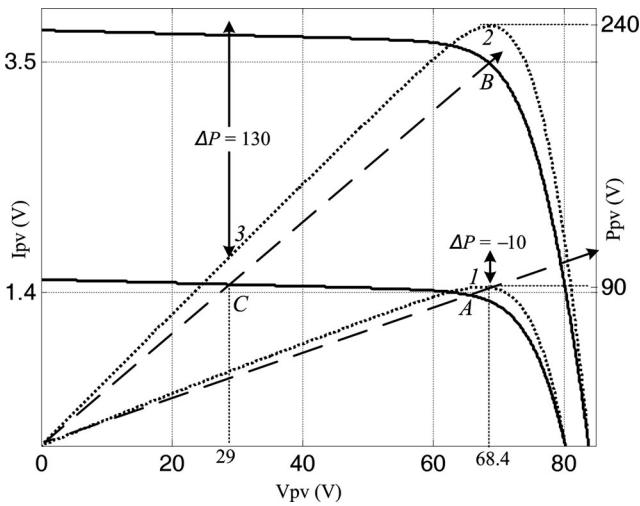


Fig. 10. $I-V$ and $P-V$ curves that are used in the simulation.

To evaluate the performance of the proposed method, comparison is made with the conventional HC. Three challenging scenarios are imposed to the system: 1) large step change in (uniform) solar insolation; 2) step change in load; and 3) partial shading conditions. These are discussed in subsequent sections.

A. Large Step Change in (Uniform) Solar Insolation

For the case of uniform change in insolation, the insolation is stepped from low to high, and then to low again. The initial level is set at $\lambda = 0.4 \text{ kW/m}^2$. At $t = 2 \text{ s}$, the insolation is suddenly stepped up to $\lambda = 1.0 \text{ kW/m}^2$. Finally at $t = 6 \text{ s}$, it is stepped down to $\lambda = 0.4 \text{ kW/m}^2$. The temperature is kept constant at 25°C . The corresponding $I-V$ and $P-V$ curves for these step changes are depicted in Fig. 10. The initial operating points for the voltage and current are labeled as point *A*. When a step-up of insolation occurs, the operating point shifts from point *A* to *B*. As a negative step change occurs, the point shifts from *B* to *C*.

Fig. 11(a) shows the simulation results for the voltage, current, duty cycle, and power, respectively obtained using the HC method. A fixed perturbation of 0.015 is imposed at every

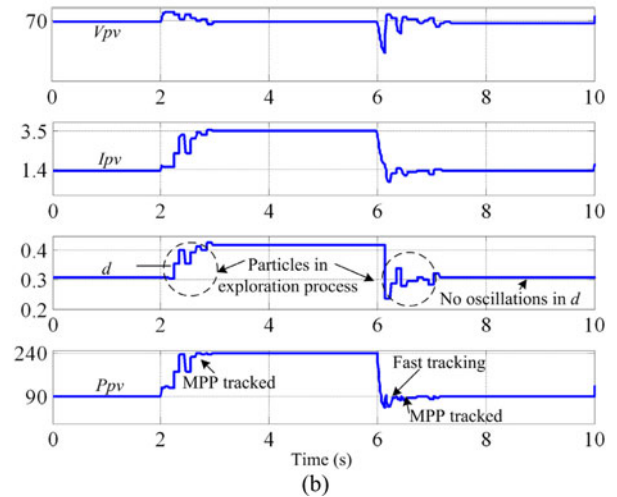
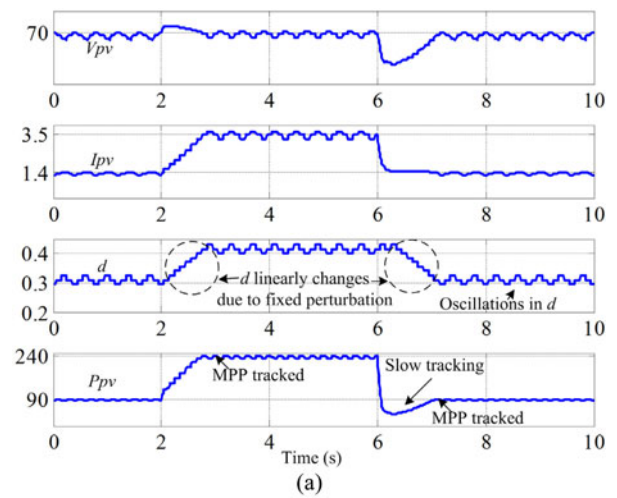


Fig. 11. Tracking voltage, current, duty cycle, and power. (a) HC method. (b) Proposed method.

0.1 s. This choice of perturbation value is based on the tradeoff between the speed of MPP tracking and the oscillation that results from the HC algorithm. As can be observed, for both step changes in insolation, the tracking is very slow. The case is more crucial when the insolation changes from $\lambda = 1.0$ to $\lambda = 0.4$

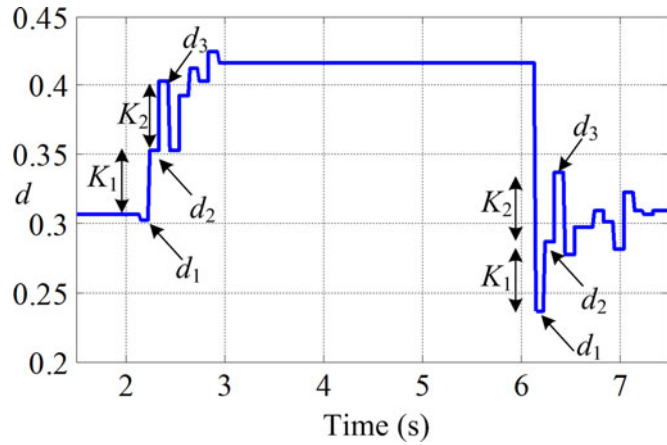


Fig. 12. Duty cycle variations during the exploring phase.

because as the operating point moves from point *B* to *C*, the PV array *PV* decreases significantly. Due to the fixed perturbation in HC, more MPPT cycles are required to reach the MPP. This is the reason for the sluggish response seen in Fig. 11(a).

More importantly, it can be clearly seen that the oscillations (in the form of ripples) around the MPP are very significant. When the insolation is maintained at $\lambda = 1$, the operating power oscillates between 240 and 231 W—a variation of 9 W. Although it is known that the oscillation can be reduced by employing a smaller duty step for the perturbation, such action would slow down the MPPT speed—particularly when the environmental fluctuation is quite large. Furthermore, if the insolation changes very rapidly, the HC method may not be able to track the changes adequately.

Fig. 11(b) shows the simulation results for the tracking voltage, current, duty cycle and power using the proposed PSO method. Additionally, a separate figure of the duty cycle is shown in Fig. 12 to provide a clearer insight on the workability of the proposed algorithm. When a step change of insolation occurs at $t = 2$ s, it results in a negative change in the operating voltage, i.e., $P - P_{old}$. Accordingly, new particles, i.e., the three duty cycles, are computed using (16) and (17). It can be observed that one of the duty cycle d_3 is very near to the final best duty cycle, as shown in Fig. 12. Using these duty cycles, searches are initiated to locate the new MPP. The exploration continuously changes the duty cycles, causing fluctuations on the voltage and current, as can be clearly observed in Fig. 11(b). At the eighth sampling interval, the algorithm correctly tracks the GP as follows: $V_{mp} = 68.4$ V and $I_{mp} = 3.5$ A, respectively. These accurately correspond to the MPP (240 W) shown in Fig. 10.

When a negative step insolation is imposed at $t = 6$ s, it results in a large change in operating power. In a similar way (to the positive step change described earlier), new duty cycles are computed using (16) and (17). Once again the algorithm demonstrates its effectiveness by locating d_2 to be very near to the final best duty cycle. Accordingly, the exploration begins until it finds the correct MPP (67 V, 1.35 A, in Fig. 10) at the ninth sampling interval. Furthermore, it can be seen that once the algorithm has successfully located the MPP and has stabilized, the oscillation

around the MPP diminishes permanently until another variation in insolation takes place. The absence of oscillation is the main feature of the proposed method.

B. Load Variation and Partial Shading

Fig. 13(a) and (b) shows the output power tracked by HC and the proposed methods, respectively, with respect to load variation and partial shading. The PV is initially operated at peak power (240 W). At $t = 2$ s, a 50% step change in load is imposed, causing a sudden drop in the operating power. Thereafter, the HC is forced to track the MPP for the new load condition; it requires ten MPPT cycles to reach the MPP. In addition, the oscillations around the MPP are very significant.

At $t = 4$ s, partial shading occurs. Consequently, the $P-V$ curves are characterized by four peaks labeled by $P1-P4$. Among these, $P1-P3$ are the local while $P4$ (170 W) are the global peaks. For HC, when the operating point changes due to partial shading, it enters the vicinity of $P3$ (144 W). It will eventually climb to this local peak and recognize it as the MPP. The difference between the true global $P4$ and the perceived peak $P3$ is 26 W or 11% of the output power. This is a very significant loss for a PV system.

In contrast, both the sudden load variation and partial shading conditions are elegantly handled by the proposed method as depicted in Fig. 13(b). When sudden load change occurs, the correct duty cycles are recalculated within five MPPT cycles. Furthermore, when the partial shading is imposed on the PV array, the algorithm explores the $P-V$ curve and successfully tracks the true global peak ($P4$) within seven MPPT cycles.

Table II qualitatively summarizes the performance of both methods. It can be seen that in general the proposed method is superior to HC with regard to dynamic performance (due to load change) and tracking speed. Moreover, it is very effective in handling the partial shading conditions. The most crucial advantage of the proposed method is its ability to eliminate the steady-state oscillations to practically zero value. However, execution wise, it takes slightly longer time to update the new duty cycle. This is to be expected because the PSO algorithm is relatively more complex than HC. Nevertheless, both methods can still be easily implemented in low-cost microcontrollers.

VI. EXPERIMENTAL RESULTS

Hardware wise, the algorithms for the MPPT controller (both the proposed and HC methods) are implemented by the Texas Instrument's TMS320F240 DSP. The platform for the software development is the DS1104 DSspace. The overall experimental set-up is based around the custom-designed PV array simulator, the PVAS2 [33]. The power stage of the PVAS2 is constructed using 20 linear MOSFETs connected in series to emulate the ripple-free PV voltage. Due to the linear power supply design of PVAS2, switching frequency ripple does not exist, hence guaranteeing noninterference between the PVAS2 with the power converter switching circuit. The $I-V$ curve is generated based on a voltage-controlled current source concept. It consists of an integrated RAM, which holds the $I-V$ curves and a microprocessor unit that provides a complete communication, monitoring

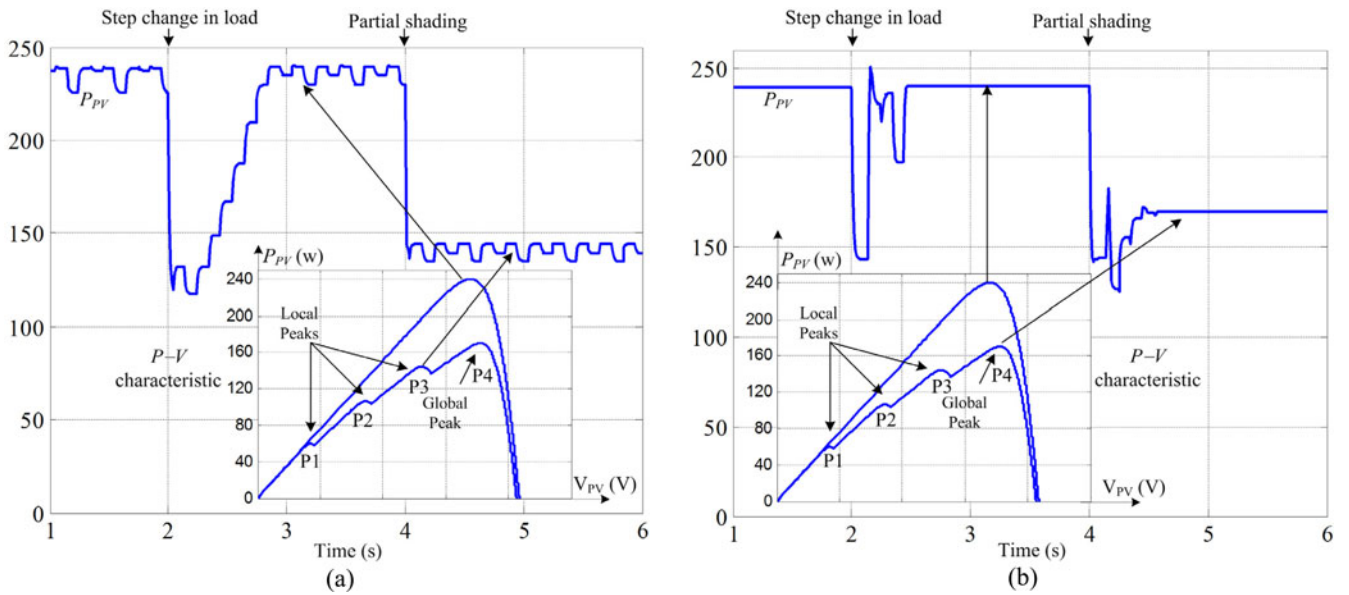


Fig. 13. Tracking performance under load variation and partial shading conditions. (a) HC method. (b) Proposed method.

TABLE II
COMPARISON OF PROPOSED PSO AND HC METHODS

Evaluated Parameters	HC Method	Proposed Method
Dynamic Performance	Poor	Good
Tracking Speed	Slow	Fast
Steady state oscillations	Large	(Practically) zero
Tracking in partial shading	Not possible	Yes
Execution time	Very fast	Fast
Practical Implementation	Yes	Yes

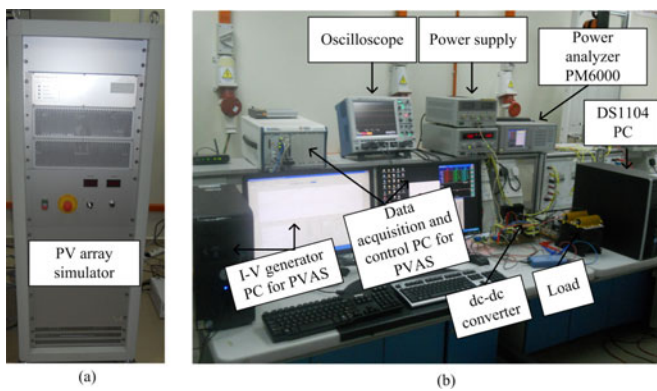


Fig. 14. (a) PVAS unit. (b) Experimental set-up of the MPPT system.

and measurement capabilities. It provides a real-time simulation capability of any time series of insolation, temperature, fill factor, or any arbitrary $I-V$ curves measured under real testing conditions. Unlike the conventional PV array simulators with diode strings, the usage of digital control and precisely defined characteristics allows the exact knowledge of MPP for every time step. Hence, a high-precision dynamic MPPT measurement can be easily achieved. The photographs of the PVAS2 and the overall experimental set-up are shown in Fig. 14(a) and (b), respectively.

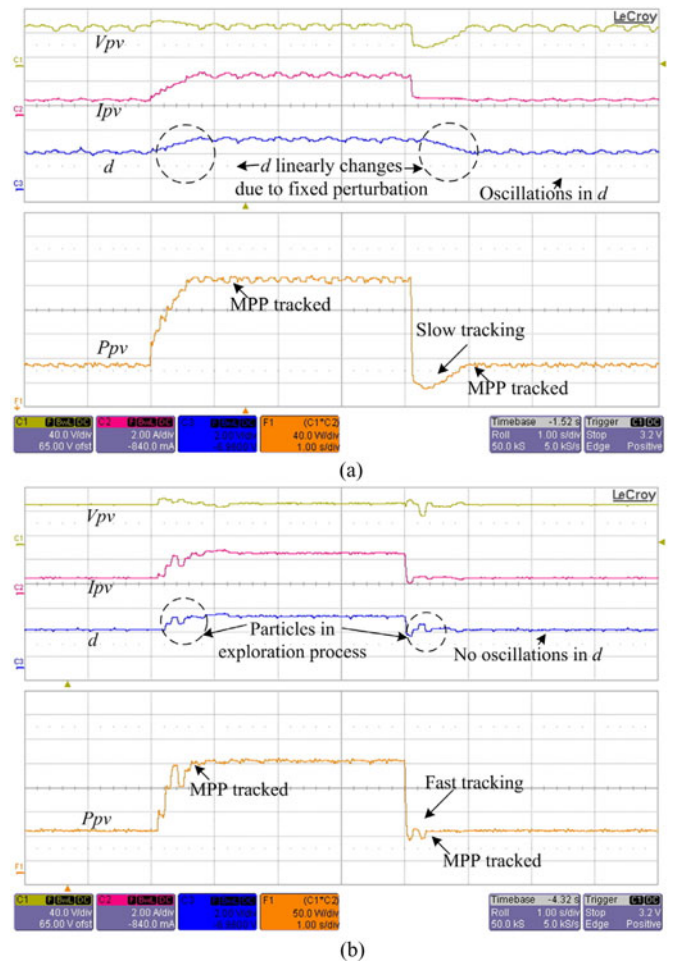


Fig. 15. Experimental waveforms: tracking voltage, current, duty cycle, and power. (a) HC method. (b) Proposed method.

Fig. 15(a) and (b) shows the experimental results for the tracking voltage, current, duty cycle, and power for HC and proposed methods, respectively. The experiments are conducted under the same conditions as described in the simulation, i.e., Section V-A. It can be seen that the experimental results match very closely to the simulation. For each operating condition, the MPP is attained in a relatively short time and exhibits almost zero oscillation in steady state. Hence, the correctness of the proposed algorithm is validated.

VII. CONCLUSION

In this paper, a PSO with the capability of direct duty cycle is used to track the MPP of a PV system. It is shown that the proposed MPPT controller exhibits an adaptive form of the HC method. To improve the tracking speed, a simple and efficient method is proposed to reinitialize the particles to search for the new MPP, resulting in superior dynamic response. The results indicate that the proposed controller outperforms the HC and gives a number of advantages: 1) it has a faster tracking speed; 2) it exhibits zero oscillations at the MPP; 3) it could locate the MPP for any environmental variations including partial shading condition and large fluctuations of insolation; and 4) the algorithm can be easily developed using a low-cost microcontrollers.

ACKNOWLEDGMENT

The authors would like to thank the Universiti Teknologi Malaysia for providing the facilities to carry out this research. The vote number for the research fund is 68704.

REFERENCES

- [1] L. Bangyin, D. Shanxu, and C. Tao, "Photovoltaic DC-building-module-based BIPV system-concept and design considerations," *IEEE Trans. Power Electron.*, vol. 26, no. 5, pp. 1418–1429, May 2011.
- [2] Z. Li, S. Kai, X. Yan, F. Lanlan, and G. Hongjuan, "A modular grid-connected photovoltaic generation system based on DC bus," *IEEE Trans. Power Electron.*, vol. 26, no. 2, pp. 523–531, Feb. 2011.
- [3] J. L. Agorreta, M. Borrega, Lo, x, J. pez, and L. Marroyo, "Modeling and control of N -paralleled grid-connected inverters with LCL filter coupled due to grid impedance in PV plants," *IEEE Trans. Power Electron.*, vol. 26, no. 3, pp. 770–785, Mar. 2011.
- [4] J. Young-Hyok, J. Doo-Yong, K. Jun-Gu, K. Jae-Hyung, L. Tae-Won, and W. Chung-Yuen, "A real maximum power point tracking method for mismatching compensation in PV array under partially shaded conditions," *IEEE Trans. Power Electron.*, vol. 26, no. 4, pp. 1001–1009, Apr. 2011.
- [5] Y. Bo, L. Wuhua, Z. Yi, and H. Xiangning, "Design and analysis of a grid-connected photovoltaic power system," *IEEE Trans. Power Electron.*, vol. 25, no. 4, pp. 992–1000, Apr. 2010.
- [6] E. Serban and H. Serban, "A control strategy for a distributed power generation microgrid application with voltage- and current-controlled source converter," *IEEE Trans. Power Electron.*, vol. 25, no. 12, pp. 2981–2992, Dec. 2010.
- [7] R. Ian H, "Envisaging feed-in tariffs for solar photovoltaic electricity: European lessons for Canada," *Renew. Sustainable Energy Rev.*, vol. 9, pp. 51–68, 2005.
- [8] L. Y. Seng, G. Lalchand, and G. M. Sow Lin, "Economic, environmental and technical analysis of building integrated photovoltaic systems in Malaysia," *Energy Policy*, vol. 36, pp. 2130–2142, 2008.
- [9] A. K. Abdelsalam, A. M. Massoud, S. Ahmed, and P. N. Enjeti, "High-performance adaptive perturb and observe MPPT technique for photovoltaic-based microgrids," *IEEE Trans. Power Electron.*, vol. 26, no. 4, pp. 1010–1021, Apr. 2011.
- [10] M. A. Masoum, H. Dehbonei, and E. F. Fuchs, "Theoretical and experimental analyses of photovoltaic systems with voltage and current-based maximum power point tracking," *IEEE Power Eng. Rev.*, vol. 22, no. 8, pp. 62–62, Oct. 2002.
- [11] T. Noguchi, S. Togashi, and R. Nakamoto, "Short-current pulse-based maximum-power-point tracking method for multiple photovoltaic-and-converter module system," *IEEE Trans. Ind. Electron.*, vol. 49, no. 1, pp. 217–223, Feb. 2002.
- [12] H. Patel and V. Agarwal, "Maximum power point tracking scheme for PV systems operating under partially shaded conditions," *IEEE Trans. Ind. Electron.*, vol. 55, no. 4, pp. 1689–1698, Apr. 2008.
- [13] S. L. Brunton, C. W. Rowley, S. R. Kulkarni, and C. Clarkson, "Maximum power point tracking for photovoltaic optimization using ripple-based extremum seeking control," *IEEE Trans. Power Electron.*, vol. 25, no. 10, pp. 2531–2540, Oct. 2010.
- [14] S. Jain and V. Agarwal, "A single-stage grid connected inverter topology for solar PV systems with maximum power point tracking," *IEEE Trans. Power Electron.*, vol. 22, no. 5, pp. 1928–1940, Sep. 2007.
- [15] K. H. Hussein, I. Muta, T. Hoshino, and M. Osakada, "Maximum photovoltaic power tracking: an algorithm for rapidly changing atmospheric conditions," *IEE Proc.-Gen., Transmiss., Dist.*, vol. 142, no. 1, pp. 59–64, Jan. 1995.
- [16] N. Femia, G. Petrone, G. Spagnuolo, and M. Vitelli, "Optimization of perturb and observe maximum power point tracking method," *IEEE Trans. Power Electron.*, vol. 20, no. 4, pp. 963–973, Jul. 2005.
- [17] A. Safari and S. Mekhilef, "Simulation and hardware implementation of incremental conductance MPPT with direct control method using cuk converter," *IEEE Trans. Ind. Electron.*, vol. 58, no. 4, pp. 1154–1161, Apr. 2011.
- [18] B. N. Alajmi, K. H. Ahmed, S. J. Finney, and B. W. Williams, "Fuzzy-logic-control approach of a modified hill-climbing method for maximum power point in microgrid standalone photovoltaic system," *IEEE Trans. Power Electron.*, vol. 26, no. 4, pp. 1022–1030, Apr. 2011.
- [19] A. K. Rai, N. D. Kaushika, B. Singh, and N. Agarwal, "Simulation model of ANN based maximum power point tracking controller for solar PV system," *Solar Energy Mater. Solar Cells*, vol. 95, pp. 773–778, 2011.
- [20] K. Ishaque and Z. Salam, "An improved modeling method to determine the model parameters of photovoltaic (PV) modules using differential evolution (DE)," *Solar Energy*, vol. 85, pp. 2349–2359, 2011.
- [21] K. Ishaque, Z. Salam, H. Taheri, and A. Shamsudin, "A critical evaluation of EA computational methods for Photovoltaic cell parameter extraction based on two diode model," *Solar Energy*, vol. 85, pp. 1768–1779, 2011.
- [22] M. Miyatake, F. Toriumi, T. Endo, and N. Fujii, "A Novel maximum power point tracker controlling several converters connected to photovoltaic arrays with particle swarm optimization technique," in *Proc. Eur. Conf. Power Electron. Appl.*, 2007, pp. 1–10.
- [23] V. Phimmasone, Y. Kondo, T. Kamejima, and M. Miyatake, "Evaluation of extracted energy from PV with PSO-based MPPT against various types of solar irradiation changes," presented at the Int. Conf. Electrical Machines and Systems, Incheon, Korea, 2010.
- [24] V. Phimmasone, T. Endo, Y. Kondo, and M. Miyatake, "Improvement of the maximum power point tracker for photovoltaic generators with particle swarm optimization technique by adding repulsive force among agents," in *Proc. Int. Conf. Electr. Mach. Syst.*, 2009, pp. 1–6.
- [25] Y. Liu, D. Xia, and Z. He, "MPPT of a PV system based on the particle swarm optimization," in *Proc. 4th Int. Conf. Electric Utility Deregulation and Restruct. Power Technol.*, 2011, pp. 1094–1096.
- [26] M. A. Hassan and M. A. Abido, "Optimal design of microgrids in autonomous and grid-connected modes using particle swarm optimization," *IEEE Trans. Power Electron.*, vol. 26, no. 3, pp. 755–769, Mar. 2011.
- [27] K. Ishaque, Z. Salam, and H. Taheri, "Simple, fast and accurate two-diode model for photovoltaic modules," *Solar Energy Mater. Solar Cells*, vol. 95, pp. 586–594, 2011.
- [28] K. Ishaque, Z. Salam, and H. Taheri, "Accurate MATLAB simulink PV system simulator based on a two-diode model," *J. Power Electron.*, vol. 11, pp. 179–187, 2011.
- [29] S. Chih-Tang, R. N. Noyce, and W. Shockley, "Carrier generation and recombination in P-N junctions and P-N junction characteristics," *Proc. IRE*, vol. 45, no. 9, pp. 1228–1243, Sep. 1957.
- [30] R. Eberhart and J. Kennedy, "A new optimizer using particle swarm theory," in *Proc. 6th Int. Symp. Micro Mach. Human Sci.*, 1995, pp. 39–43.
- [31] K. Ishaque, Z. Salam, H. Taheri, and Syafaruddin, "Modeling and simulation of photovoltaic (PV) system during partial shading based on a

two-diode model,” *Simul. Modelling Pract. Theory*, vol. 19, pp. 1613–1626, 2011.

- [32] D. Sera, R. Teodorescu, J. Hantschel, and M. Knoll, “Optimized maximum power point tracker for fast-changing environmental conditions,” *IEEE Trans. Ind. Electron.*, vol. 55, no. 7, pp. 2629–2637, Jul. 2008.
- [33] *User’s Manual*, “Programmable Photovoltaic Array Simulator PVAS1,” Arsenal Research, AIT Austrian Institute of Technology, Australia, 2007.



Kashif Ishaque received the B.E. degree in Industrial Electronics Engineering from the Institute of Industrial Electronics Engineering, NEDUET, Karachi, Pakistan, in 2007, and the Master of Engineering Science and Ph.D. degrees from Universiti Teknologi Malaysia Johor Bahru, Malaysia, in 2009 and 2012 respectively.

He is currently an Assistant Professor at the Department of Electronics Engineering, PAF Karachi Institute of Economics and Technology (PAF-KIET), Karachi. He is the author or coauthor of more than 30

publications in international journals and proceedings. His research interests include photovoltaic modeling and control, intelligent control, nonlinear systems control, and optimization techniques such as genetic algorithm, particle swarm optimization, and differential evolution.



Zainal Salam (M’11) received the B.S., M.E., and Ph.D. degrees from the University of California, Oakland; Universiti Teknologi Malaysia (UTM), Johor Bahru, Malaysia; and the University of Birmingham, U.K., in 1985, 1989, and 1997, respectively.

He was a Lecturer at UTM for 24 years and is now a Professor of Power Electronics in the School of Electrical Engineering. He has been involved on several research and consulting projects in the area of battery-powered converters. He is currently the Director of the Inverter Quality Control Center, UTM,

where he is responsible for testing PV inverters that are to be connected to the local utility grid. His research interests include all areas of power electronics, renewable energy, power electronics, and machine control.



Muhammad Amjad received the B.Sc. and M.Sc. degrees in Electrical Engineering from the University of Engineering and Technology, Lahore, Pakistan, in 1998 and 2006, respectively. He is currently working toward the Ph.D. degree in Electrical Engineering from Universiti Teknologi Malaysia, Johor Bahru, Malaysia.

He was a Lecturer at the University College of Engineering and Technology, TheIslamia University of Bahawalpur, Punjab, Pakistan, for 10 years. His research interests include modeling of dielectric barrier discharge (DBD) chamber and power electronic converter for DBD applications.



Saad Mekhilef (M’01) received the B.Eng. degree in Electrical Engineering from the University of Setif, Setif, Algeria, in 1995, and the Master of Engineering Science and Ph.D. degrees from the University of Malaya, Kuala Lumpur, Malaysia, in 1998 and 2003, respectively.

He is currently a Professor at the Department of Electrical Engineering, University of Malaya, Kuala Lumpur. He is the author or coauthor of more than 150 publications in international journals and proceedings. He is actively involved in industrial consultancy, for major corporations in the power electronics projects. His research interests include power conversion techniques, control of power converters, renewable energy, and energy efficiency.